Organophosphorus Hydrolase Is a Remarkably Stable Enzyme That Unfolds through a Homodimeric Intermediate†

Janet K. Grimsley,‡ J. Martin Scholtz,‡,§ C. Nick Pace,‡,§ and James R. Wild*,‡

Department of Biochemistry & Biophysics and Department of Medical Biochemistry and Genetics, and Center for Macromolecular Design, Texas A&M University, College Station, Texas 77843-2128

Received July 2, 1997; Revised Manuscript Received September 18, 1997⊗

ABSTRACT: Organophosphorus hydrolase (OPH, EC 8.1.3.1) is a homodimeric enzyme that catalyzes the hydrolysis of organophosphorus pesticides and nerve agents. We have analyzed the urea- and guanidinium chloride-induced equilibrium unfolding of OPH as monitored by far-ultraviolet circular dichroism and intrinsic tryptophan fluorescence. These spectral methods, which monitor primarily the disruption of protein secondary structure and tertiary structure, respectively, reveal biphasic unfolding transitions with evidence for an intermediate form of OPH. By investigating the protein concentration dependence of the unfolding curves, it is clear that the second transition involves dissociation of the monomeric polypeptide chains and that the intermediate is clearly dimeric. The dimeric intermediate form of OPH is devoid of enzymatic activity, yet clearly behaves as a partially folded, dimeric protein by gel filtration. Therefore, we propose an unfolding mechanism in which the native dimer converts to an inactive, well-populated dimeric intermediate which finally dissociates and completely unfolds to individual monomeric polypeptides. The denaturant-induced unfolding data are described well by a three-state mechanism with ΔG for the interconversion between the native homodimer (N_2) and the inactive dimeric intermediate (I_2) of 4.3 kcal/mol while the overall standard state stability of the native homodimer relative to the unfolded monomers (2U) is more than 40 kcal/mol. Thus, OPH is a remarkably stable protein that folds through an inactive, dimeric intermediate and will serve as a good model system for investigating the energetics of protein association and folding in a system where we can clearly resolve these two steps.

Equilibrium denaturation studies have provided detailed knowledge concerning the structure, stabilization, and folding of small, monomeric proteins. A general understanding of the forces involved in protein stability will require investigations of multisubunit proteins, where additional modes of stabilization are available at the quaternary structural level. These studies will also enhance our knowledge concerning energetic and structural aspects of oligomer formation. The structures of intermediates that form on the folding pathway will provide valuable information about folding pathways. There are numerous examples of monomeric intermediates that are significantly populated during the equilibrium denaturation of a dimer (*1*−*8*); however, dimeric intermediates are rare (*9*−*11*). To date, the best structural information and thermodynamic data concerning dimeric folding intermediates come from studies of bacterial luciferase (*10*), and the *Escherichia coli Trp* repressor (*11*).

We have begun to study the folding of bacterial organophosphorus hydrolase (OPH),[1] a dimeric metalloenzyme (M_r = 72 000$_{dimer}$) from *Pseudomonas diminuta* which contains 336 residues per monomer (*12*−*13*) (Figure 1). This enzyme has received considerable attention focusing on its use as a bioremediation agent. OPH has broad substrate specificity. It can catalyze the breakdown of several insecticides (paraoxon, parathion, coumaphos) with surprisingly high rates (10^4 s^{-1} for paraoxon) and nerve agents such as soman, sarin (*14*−*15*), and VX [*O*-ethyl *S*-(2-diisopropylaminoethyl)methylphosphonothiolate] (*16*). The active site of OPH consists of a binuclear metal center that can bind several metals, including Zn^{2+}, Co^{2+}, Mn^{2+}, Cd^{2+}, or Ni^{2+} (*17*). These metals are involved in catalysis and structural functions. The gene encoding OPH has been cloned and the protein expressed in *Escherichia coli* (*18*). The purification procedure for OPH has also been reported (*17*) and is modified in this report (see Experimental Procedures). In addition, recent crystallographic investigations have provided structural and functional details concerning the enzymatic mechanism of this enzyme (*19*−*21*).

OPH is unique among other organophosphate degrading enzymes because it can hydrolyze phosphofluoridates, such as soman and sarin, and the phosphothioates such as VX, which constitute the major chemical warfare deterrents stockpiled by the United States and the Former Soviet Union. Development of an efficient and safe detoxification procedure for organophosphorus nerve agents and various environmental pollutants will be of great value.

Practical applications for bioremediation will require enzymes with enhanced structural stability and improved catalytic efficiency. Significant improvement of the activity and substrate specificity has been achieved through site-directed mutagenesis of histidinyl residues affecting the metal content and modifying the boundaries of the active site.

†This study was supported by an ARO University Initiative (Grant DAAL 03-92-G-0171) with Texas A&M University, and the Texas Agricultural Experimental Station of The Texas A&M University System. J.M.S. is an American Cancer Society Junior Faculty Research Awardee (JFRA-577).

* To whom correspondence should be addressed.

‡ Department of Biochemistry & Biophysics.

§ Department of Medical Biochemistry and Genetics.

⊗ Abstract published in *Advance ACS Abstracts,* November 1, 1997.

[1] Abbreviations: OPH, organophosphorus hydrolase; GdmCl, guanidinium chloride; CD, circular dichroism; Fl, fluorescence spectroscopy.

S0006-2960(97)01596-1 CCC: $14.00 © 1997 American Chemical Society

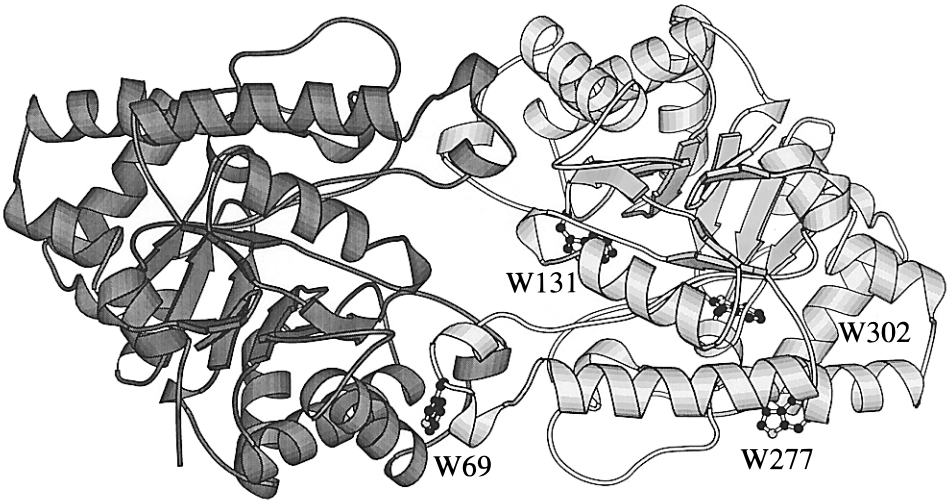

FIGURE 1: Ribbon drawing of OPH. The drawing was generated from the crystal structure of OPH (*19*) using MOLSCRIPT (*25*). The two halves of the dimer are shaded differently, and in the subunit with lighter shading, the four Trp residues per monomer are shown. The crystallographic 2-fold rotational axis is perpendicular to the plane of the page.

Individual enzymes have demonstrated dramatic improvement in activity against various organophosphorus neurotoxins (*22*−*24*). Many of these modified enzymes retain excellent catalytic activity and specificity for preferred substrates, despite the loss of one of the two molecules of a metal present in each subunit. These results demonstrated that only a single metal is required for enzymatic function and suggested that the changes in catalytic metal geometries are associated with the alteration of substrate specificities.

OPH utility in the remediation of hazardous compounds is compromised by our limited understanding of its stability and how the enzyme would behave in environments most typical of where it would be used. Since OPH is insoluble in organic solvents which are suitable for solubilization of nerve agents, enzyme-based detoxification of bulk nerve agents (for instance in an existing war head or a concentrated spill of pesticide) must often rely on the use of OPH in biphasic mixtures. This fact points to the first challenge: In order to efficiently function in detoxification of bulk nerve agents, OPH must be stable in the presence of organic solvents. In order to increase the productivity of the process, we must immobilize the enzyme in the most effective way currently available. This points to the next challenge: OPH must have the highest possible stability under adverse conditions. Key to the realization of this goal is a detailed analysis of the thermodynamic stability of OPH.

We report here the urea- and guanidinium chloride-induced unfolding of Zn-containing OPH monitored at equilibrium using spectroscopic methods that are sensitive to protein secondary and tertiary structure. Fluorescence emission was monitored after excitation at 278 nm, allowing excitation of both tyrosinyl and tryptophanyl residues. Each subunit of OPH has four tryptophanyl residues (Figure 1) and four tyrosinyl residues. One of these, Trp 69, is located at the subunit interface. Trp 302, Trp 131, and Tyr 239 are located near the active site "histidine cluster" (*19*). As a result, fluorescence spectroscopy should be a powerful tool to monitor conformational changes of this enzyme, even at the active site. We also monitored circular dichroism at 230 nm and enzymatic activity. These data demonstrate that the unfolding of OPH occurs by a three-step process that includes an inactive dimeric intermediate. The conformational stability determined in this study is the highest for any dimeric protein reported so far.

EXPERIMENTAL PROCEDURES

Materials. Ultra-pure urea and all buffer components were purchased from Sigma, St. Louis, MO. Ultra-pure guanidinium chloride (GdmCl) was purchased from USB, Cleveland, OH. Tryptone and yeast extract were purchased from Fisher Scientific, Pittsburgh, PA. Phosphoglucose isomerase, carbonic anhydrase, and glutathione transferase were purchased from Sigma. Bacterial organophosphorus hydrolase was expressed from *Escherichia coli* DH5α (supE44 ΔlacU169 [Φ80 lacZΔM15] hsdR17 recA1 endA1 gryA96 thi-1 relA1) carrying the plasmid pUC19-opd as described previously (*26*).

Protein Purification. E. coli DH5α cells with pUC19-opd were grown in enriched media containing 24 g of yeast extract/L, 12 g of tryptone/L, 100 mM K_2HPO_4/KH_2PO_4, pH 7.0, 0.4% glycerol, and 1 mM $CoCl_2$ for 40 h at 30 °C and supplemented with 50 μg/mL ampicillin. Cells were harvested and resuspended in 10 mM phosphate buffer, pH 6.9 (40 g was resuspended in 160 mL of buffer). All buffers used during the purification contained 50 μM zinc acetate. Cells were disrupted by sonication on ice, and the cell-free extract was subjected to 1% streptomycin sulfate precipitation to remove bulk nucleic acids. This was followed by 45% ammonium sulfate precipitation. The protein precipitate was resuspended in ~40 mL of phosphate buffer and dialyzed against the same buffer. This dialysate was loaded onto a 100 mL SP-Sepharose column at a flow rate of 1 mL/min equilibrated in phosphate buffer. The column was washed extensively until the optical density at 280 nm was <0.05, at which time a linear potassium chloride gradient (500 mL) from 0 to 0.5 M in 10 mM phosphate buffer, pH 6.9, was initiated. OPH begins to elute at around 125 mM KCl. OPH-containing fractions were pooled and dialyzed against 10 mM Tris, pH 8.3, and loaded onto a 10 mL DEAE-Sephacel column at a flow rate of 2−3 mL/min equilibrated in the same buffer (this step can be performed at room temperature with little effect on activity). Under these conditions, OPH passes directly through the column. OPH-containing fractions were pooled, concentrated to 2 mg/mL, and used

immediately in protein folding studies. Remaining protein was stored at −20 °C in the presence of 30% glycerol. The purity of OPH was determined by SDS−polyacrylamide gel electrophoresis with Coomassie Blue staining. Zinc content was determined by flame atomic absorption spectrophotometry on a Perkin-Elmer 2380 atomic absorption spectrophotometer.

Stock Solutions. Urea and GdmCl stock solutions (approximately 10 M and 4 M, respectively) were prepared as described by Pace *et al.* (*27*) in a buffer of 10 mM Tris, pH 8.3. The denaturant concentrations of each stock solution were calculated by weight and by refractive index (*27*). These solutions were used in subsequent experiments only if the difference between these two values was less than 1%.

Equilibrium Unfolding Curves. All equilibrium unfolding experiments in denaturant were performed as described by Pace *et al.* (*27*). Stock protein solutions were prepared in Tris buffer to be 16 times the desired final protein concentration. Buffer, urea, or GdmCl from the concentrated stocks and 200 μL of stock protein solution to give a final volume of 3.2 mL were added to disposable 12 × 75 mm borosilicate glass tubes (Fisher Scientific). The final urea and GdmCl concentrations ranged from 0 to 9 M and from 0 to 4 M, respectively. The final protein concentrations were as indicated in the figure legends. All denaturation curves were done in duplicate. Each sample was mixed gently immediately after adding protein by inverting the tube 4−5 times. All samples were then incubated in a water bath at 25 °C for a minimum of 24 h. This was shown to be sufficient time to reach equilibrium. To test for reversibility, a solution of protein in the posttransition region of the denaturation curve was diluted with protein and buffer in the pretransition region, and fluorescence intensity was then measured directly. Enzyme activity was also used as a measure of reversibility.

We used 278 nm as the excitation wavelength for fluorescence spectroscopy allowing excitation of both tyrosinyl and tryptophanyl residues. The emission wavelength was 320 nm, where the maximum difference in fluorescence between the native and denatured protein occurred. The fluorescence emission at each denaturant concentration was measured using an SLM-Aminco 8000C spectrofluorometer. The signal was averaged for 39 s. All measurements were corrected for background signals contributed by either buffer or denaturant. Circular dichroism was measured using an Aviv 62DS spectropolarimeter. The CD signal was averaged for 60 s. Both instruments were equipped with thermostatted cell holders, and the temperature was held constant at 25 °C.

Data Analysis. For a two-state unfolding transition, only the folded and unfolded conformations are present at significant concentrations for any of the points shown on a denaturation curve from low denaturant concentration to a high concentration. Therefore, the fraction of folded protein plus the fraction of unfolded protein will be equal to 1. The fraction of folded and unfolded protein can then easily be determined based on the observed values of the spectroscopic signal along the curve, and the values associated with the folded and unfolded forms. Knowing the fraction of each species present at each denaturant concentration, the equilibrium constant, K, and the free energy change, ΔG, can be calculated (*28*). It has been shown for many proteins (*29*, *30*) that ΔG varies linearly with denaturant concentration, at least in the transition region. The simplest method of estimating the conformational stability is to assume that the linear dependence continues to zero denaturant concentration and to use a least-squares analysis to fit the data to the equation:

$$\Delta G = \Delta G_{\mathrm{W}} - m[\mathrm{denaturant}]$$

where ΔG_{W} is the conformational stability without denaturant and m is a measure of the dependence of ΔG on denaturant concentration. It has been shown that the m value is a measure of the ability of the denaturant to unfold a protein (*28*) and is proportional to the amount of protein surface area exposed upon unfolding (*31*). One unifying equation is used to analyze an entire denaturation curve (*28*, *32*), and the unknown parameters are determined by a nonlinear least-squares program.

Our experimental unfolding data could not be reconciled to a simple two-state mechanism. There are two separate transitions: one from the native dimeric protein to an intermediate and the second from the intermediate to completely unfolded subunits. Analysis of a three-state unfolding mechanism obviously requires more parameters. In addition, since OPH is a homodimer, some reactions are not unimolecular, and the equilibrium populations of folded and unfolded protein are dependent on protein concentration. For the case where a single homodimeric intermediate is in equilibrium with the native enzyme and the unfolded subunits:

$$\mathrm{N_2} \leftrightarrow \mathrm{I_2} \leftrightarrow 2\mathrm{U} \tag{1}$$

a three-state model developed by Clark *et al.* (*10*) can be employed. This model assumes that the protein is either in the native homodimeric state (N_2), in an inactive dimeric state (I_2), or in the unfolded monomeric state (U). If we set the molar concentration of the native homodimer $[N_2] = [P]_T$ when all the protein is native, we can define the mole fraction of each species as

$$f_{\mathrm{N}} = [\mathrm{N_2}]/[\mathrm{P}]_{\mathrm{T}} \tag{2}$$

$$f_{\mathrm{I}} = [\mathrm{I_2}]/[\mathrm{P}]_{\mathrm{T}} \tag{3}$$

$$f_{\mathrm{U}} = [\mathrm{U}]/[\mathrm{P}]_{\mathrm{T}} \tag{4}$$

where f_N = mole fraction in the native state, f_I = mole fraction in the intermediate homodimeric state, and f_U = mole fraction in the denatured state. Therefore

$$f_{\mathrm{N}} + f_{\mathrm{I}} + f_{\mathrm{U}} = 1 \tag{5}$$

We can now relate the equilibrium constants for the unfolding reaction (K_1 and K_2) to the mole fraction of each species present and the total protein concentration $[P]_T$ by the equations:

$$K_1 = f_{\mathrm{I}}/f_{\mathrm{N}} \tag{6}$$

and

$$K_2 = [\mathrm{P}]_{\mathrm{T}} f_{\mathrm{U}}{}^2/f_{\mathrm{I}} \tag{7}$$

where f_N, f_I, and f_U represent the fraction of the protein that is in each form at equilibrium.

By rearranging and combining eqs 5 and 6, the following is obtained:

$$f_I = K_1(1 - f_U)/(1 + K_1) \quad (8)$$

It is now possible to solve for the mole fraction of each species at equilibrium in terms of the total protein concentration, $[P]_T$, and the two equilibrium constants (K_1 and K_2). Substituting eq 8 into eq 7 and solving for f_U give the equation:

$$f_U = -K_1K_2 + \sqrt{(K_1K_2)^2 + 4[P]_T(1 + K_1)(K_1K_2)}/2[P]_T(1 + K_1) \quad (9)$$

Substituting eq 9 into eq 8 gives the equation:

$$f_I = K_1\{2[P]_T(1 + K_1) + K_1K_2 - \sqrt{(K_1K_2)^2 + 4[P]_T(1 + K_1)(K_1K_2)}/2[PT](1 + K_1)^2\} \quad (10)$$

Finally, we can substitute eq 10 into eq 6, giving us the equation:

$$f_N = 2[P]_T(1 + K_1) + K_1K_2 - \sqrt{(K_1K_2)^2 + 4[P]_T(1 + K_1)(K_1K_2)}/2[PT](1 + K_1)^2 \quad (11)$$

From eqs 6, 7, and 9−11 and the relationship

$$\Delta G = -RT \ln K_{eq} \quad (12)$$

where R is the gas constant and T is the temperature in degrees kelvin, we may now calculate the equilibrium constant and the value of ΔG at each denaturant concentration. We assumed the free energy change for each step in the reaction to be linearly dependent on denaturant concentration as described above:

$$\Delta G_1 = \Delta G1_W - m_1[\text{denaturant}] \quad (13)$$

and

$$\Delta G_2 = \Delta G2_W - m_2[\text{denaturant}] \quad (14)$$

where $\Delta G1_W$ and $\Delta G2_W$ are the free energy changes in the absence of denaturant corresponding to steps K_1 and K_2, respectively, and m_1 and m_2 are the denaturant m values. Alternative methods for the analysis of solvent denaturation curves, which include those that describe a nonlinear dependence of ΔG on the molar concentration of denaturant, require additional parameters. Here we elect to use the simplest expression, the linear extrapolation method, to minimize the total number of parameters needed to describe our data.

The amplitude of the spectroscopic signal determined at each urea concentration was assumed to be a linear combination of the fractional contribution from each species:

$$Y = Y_N f_N + Y_I f_I + Y_U f_U \quad (15)$$

where Y_N, Y_I, and Y_U are the amplitudes of the signals for the respective species. The amplitudes associated with the native and unfolded forms of the protein were also assumed to be linearly dependent on urea concentration such that

$$Y_N = Y_{N^\circ} + b_1[\text{denaturant}] \quad (16)$$

and

$$Y_U = Y_{U^\circ} + b_2[\text{denaturant}] \quad (17)$$

where Y_{N° and Y_{U° are the amplitudes of the signals in the absence of denaturant for the native and unfolded proteins, respectively, and b_1 and b_2 are the slopes that describe the dependence of the amplitudes for native and unfolded protein, respectively, on denaturant concentration. Again to minimize the total number of parameters needed, we have assumed that Y_I (and for the CD data, Y_U) does not vary with denaturant concentration.

Nonlinear least-squares fitting of the above equations to the data employed a Macintosh version of *Nonlin* (Robelko Software, Carbondale, IL; *33*) to determine the nine unknown parameters: $\Delta G1_W$ and $\Delta G2_W$ (conformational stabilities of the first and second unfolding transitions, respectively), m_1 and m_2 (m values for the first and second unfolding transitions, respectively), b_1 and b_2 (slopes for the pre- and posttransition base lines, respectively), and Y_{N°, Y_{U°, and Y_I (spectroscopic signals contributed by the native, unfolded, and intermediate forms of the protein). For the CD data, we were also able to perform a global analysis of the denaturation data collected over the range of protein concentrations, using protein concentration as an additional constant in the analysis. A global analysis of the fluorescence data could not be performed, since our fluorescence measurements only give relative changes in intensity, not absolute changes, and this varies for each experiment and also depends on the total amount of protein present in the cell.

Enzymatic Activity Measurements. Enzymatic activity was measured by monitoring the change in absorbance at 400 nm when 1.0 mM paraoxon was hydrolyzed to diethyl phosphate and *p*-nitrophenolate anion (ϵ_{400} = 17 000 M^{-1} cm^{-1}) in 20 mM CHES buffer, pH 9.0, at 25 °C (*22*) using a Gilford Response UV−VIS spectrophotometer. Paraoxon was purified as described previously (*22*).

Thermal Denaturation Monitored by Circular Dichroism. Circular dichroism measurements were performed using a Jasco J600A spectropolarimeter. Thermal denaturation was monitored by measuring circular dichroism at 230 nm in 1.0 °C steps. The samples equilibrated for 1 min at each temperature, and the signal was recorded for 30 s. This rate of heating was adequate to achieve equilibrium at each temperature. OPH unfolding was only partially reversible under these conditions, so no attempt was made to obtain a thermodynamic characterization of the thermal unfolding.

RESULTS

Equilibrium Unfolding of OPH. In general, for dimeric proteins, the overall unfolding reaction must start with the folded dimer (N_2) and end with two unfolded monomers (2U). There are, however, several possible ways this can occur:

$$\text{Case 1: } N_2 \Leftrightarrow 2U$$

In this case, one expects monophasic unfolding curves, superimposable for all spectroscopic probes used to monitor unfolding at a fixed protein concentration. The basis for the thermodynamic analysis is the assumption that only two

states, the native dimer and denatured monomers, exist at equilibrium (*34*, *35*):

$$\text{Case 2: } N_2 \leftrightarrow 2N \text{ (or } 2I) \leftrightarrow 2U$$

$$\text{Case 3: } N_2 \leftrightarrow I_2 \leftrightarrow 2U$$

The situation is quite different for cases 2 and 3. Here, one expects biphasic unfolding curves and/or nonsuperimposable transitions if the spectral probes (CD or fluorescence) used are differentially sensitive to the various species. In these instances, a general three-state model of equilibrium dissociation and unfolding would involve a native dimer (N_2), unfolded monomer (U), native monomer (N), and either a monomeric (I) or a dimeric (I_2) intermediate. The ability to distinguish between case 2 and case 3 depends on which step is protein concentration-dependent, and hence bimolecular. If the first step is bimolecular, subunit dissociation is occurring, and the intermediate is monomeric. However, if the second step is protein concentration-dependent, subunit dissociation occurs only after formation of the dimeric intermediate. The dependence of the unfolding behavior on protein concentration is the unique characteristic of coupled denaturation and dissociation of oligomeric protein systems and is used as a definitive criterion for assigning the unfolding mechanism as well as for evaluating the thermodynamic parameters (*36*).

The equilibrium unfolding of OPH was investigated by monitoring the changes in the intrinsic tryptophan fluorescence at 320 nm and the circular dichroism at 230 nm, using GdmCl as denaturant. Figure 2A shows typical unfolding curves for OPH at the highest protein concentration used in these experiments (125 μg/mL). Four separate denaturation curves were performed from different protein preparations, demonstrating the reproducibility of these data. The pronounced plateau near 1.6 M GdmCl observed for both spectroscopic probes clearly indicates the presence of a folding intermediate. However, in some experiments, we observed that the protein tends to precipitate at low GdmCl concentrations. This problem did not occur when urea was used as the denaturant, so we used urea for all of the subsequent experiments that were used to determine the stability of the enzyme.

The equilibrium unfolding curves using urea as denaturant are shown in Figure 2B. With fluorescence, the reduction in tertiary structure was clearly biphasic. However, this was not as obvious in the unfolding curves followed by CD. The noncoincidence of the transitions monitored by fluorescence and CD is clearly evident, indicating that OPH unfolding is not a simple two-state process. The reversibility of the urea-induced unfolding transition was shown spectroscopically and by quantitative (>85%) recovery of enzyme activity following refolding by dilution (data not shown).

Fluorescence Spectra. The spectral changes associated with the denaturation of OPH were studied by fluorescence. Figure 3A shows the fluorescence emission spectra of native OPH (in 0 M GdmCl), the folding intermediate (in 1.6 M GdmCl), and denatured OPH (in 4 M GdmCl). The fluorescence maximum was shifted under these conditions from 331 nm, to 337 nm, and finally to 353 nm, respectively. The fluorescence emission spectra with urea as denaturant were not significantly different (data not shown). The

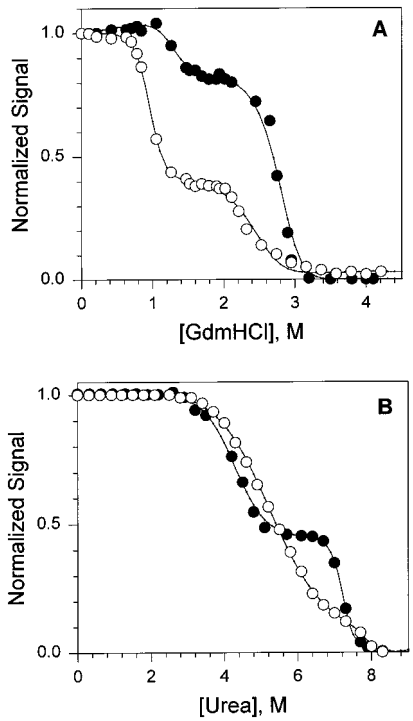

FIGURE 2: GdmCl-induced unfolding of OPH and noncoincidence of equilibrium unfolding data. (A) GdmCl-induced unfolding of OPH (125 μg/mL) was measured by fluorescence emission (●) at 320 nm with excitation at 278 nm and by CD (○) at 230 nm. (B) Urea-induced unfolding of OPH (125 μg/mL) was measured by fluorescence emission (●) at 320 nm with excitation at 278 nm and by CD (○) at 230 nm. Theoretical curves for (B) were calculated using the appropriate thermodynamic parameters in Table 1. These parameters were obtained from a nonlinear least-squares fit of the equations shown under Experimental Procedures to the indicated data.

fluorescence data indicated that OPH was largely unfolded in the presence of 4 M GdmCl, (or 8 M urea) 10 mM Tris, pH 8.3, and was complete within 12 h with no further change in the spectrum observed.

Circular Dichroism Spectra. The molecular architecture of the native enzyme is a distorted α/β barrel with 8 parallel β-strands forming the barrel and linked on the outer surface by 14 α-helices (*19*). The far-UV CD spectrum of native OPH displayed a double minimum around 210 and 222 nm, typical of a protein with high α-helical content (Figure 3B), consistent with the known three-dimensional structure. Upon complete denaturation in 4 M GdmCl, there was a large decrease in CD intensity, indicating loss of secondary structure. The folding intermediate (in 1.6 M GdmCl) possesses about 50% of the native CD spectral amplitude at 222 nm. The CD spectra with urea as denaturant were not significantly different (data not shown).

Effect of OPH Concentration on the Unfolding Transition. Since OPH is a homodimer, we determined the concentration dependence of the unfolding process. We observed that the biphasic nature of unfolding was more pronounced at the highest protein concentration when unfolding was followed by fluorescence (Figure 4). As the protein concentration increased, there was a shift in the position of the midpoint of the second unfolding transition to higher urea concentrations. The fluorescence results suggest that subunit dissociation was occurring in the second step of the unfolding process. No concentration dependence was observed between 0 and 4 M urea. These results support the three-state

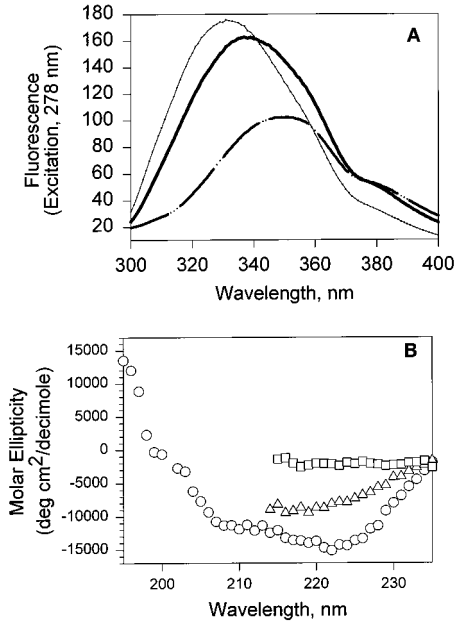

FIGURE 3: Fluorescence and circular dichroism spectra of native OPH, the folding intermediate, and denatured OPH. (A) Fluorescence spectra at 25 °C of 125 μg/mL native OPH in 10 mM Tris, pH 8.3 (thin solid line), 10 mM Tris, pH 8.3, 1.6 M GdmCl (heavy solid line), and 10 mM Tris, pH 8.3, 4 M GdmCl (dashed line). (B) CD spectra at 25 °C of 125 μg/mL native OPH in 10 mM Tris, pH 8.3 (○), 10 mM Tris, pH 8.3, 1.6 M GdmCl (△), and 10 mM Tris, pH 8.3, 4 M GdmCl (□).

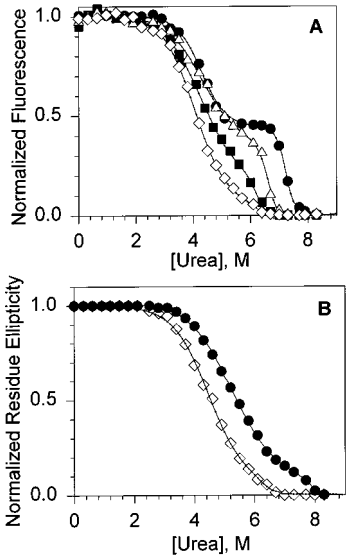

FIGURE 4: Dependence of equilibrium unfolding of OPH on protein concentration. (A) Unfolding was monitored by fluorescence emission at 320 nm with excitation at 278 nm at protein concentrations of 12.5 μg/mL (◇), 34 μg/mL (■), 68 μg/mL (△), and 125 μg/mL (●). (B) Unfolding was monitored by CD at 230 nm at protein concentrations of 12.5 μg/mL (◇) and 125 μg/mL (●). Theoretical curves were calculated using the appropriate thermodynamic parameters in Table 1. These parameters were obtained from a nonlinear least-squares fit of the equations shown under Experimental Procedures to the data.

mechanism:

$$N_2 \Leftrightarrow I_2 \Leftrightarrow 2U$$

in which a homodimeric intermediate is well-populated. If this model provides a reasonable thermodynamic description of the denaturation reaction, then we expect the same value for the conformational stability from experiments performed at different protein concentrations, irrespective of the probe used to monitor the transition(s). In the analysis of the separate denaturation experiments, we find that ΔG_W values that are nearly identical over the protein concentration range used in these experiments (Table 1) regardless of which probe is used to monitor the transitions. Furthermore, a global analysis of the unfolding data as monitored by CD for the entire range of protein concentration revealed identical parameters to those found from the individual analyses (Table 1), supporting the model employed. The free energy change, $\Delta G1_W$, and the denaturant m value, m_1, associated with the first step in urea denaturation were 4.3 kcal/mol and 0.95 kcal mol^{-1} M^{-1}, respectively. No subunit dissociation seems to occur in this first phase of unfolding. The second step in unfolding involves subunit dissociation of OPH and the transition from a stable, partially-folded dimeric intermediate to two unfolded subunits. The free energy change, $\Delta G2_W$, and the denaturant m value, m_2, of this step were also relatively constant over the protein concentration range used. These values were 37.8 kcal/mol and 4.5 kcal mol^{-1} M^{-1}, respectively.

The dimeric nature of the intermediate was also confirmed by gel filtration (data not shown). At urea concentrations where the intermediate is well-populated, OPH elutes from the column at the correct size for a dimer, suggesting that higher order species are not contributing to the equilibrium unfolding of OPH. This result is consistent with the analysis of the unfolding transitions observed by our spectroscopic probes.

Loss of Enzymatic Activity upon Unfolding. We used enzymatic activity to monitor the denaturation of OPH in addition to the spectroscopic methods. Assays were done on the same samples that were used in the folding experiments. These data illustrate that the intermediate is not active when paraoxon is used as substrate in the assay (Figure 5). An analysis of data such as these led to the results in Table 2. The midpoint of the denaturation curve occurred at about 3.77 M urea and was independent of protein concentration. The values of ΔG_W and m, for a two-state transition, were 4.3 kcal/mol and 1.14 kcal mol^{-1} M^{-1}, respectively, in good agreement with the parameters for the first step in unfolding determined from spectroscopic measurements (Table 1). The experiments support the idea that the intermediate is a dimer and that it is inactive.

Thermal Denaturation of OPH. In addition to the urea and GdmCl denaturation, we used temperature to induce the denaturation of OPH (data not shown). Unfortunately, thermal denaturation was not reversible due to protein aggregation at high temperatures. However, the relatively high apparent T_m observed (≈75 °C) confirmed that OPH is a very heat-stable protein.

DISCUSSION

The nonsuperimposable transitions observed with different spectroscopic probes and the biphasic nature of the unfolding denaturation curve (Figure 2) are consistent with the existence of a stable folding intermediate. At the OPH concentrations used in this work, native OPH is dimeric. The remaining question was whether the unfolding intermediate was monomeric or dimeric. The first unfolding transition from native dimer to intermediate (0−4.5 M urea) was

Table 1: Thermodynamic Parameters Obtained from Urea Equilibrium Denaturation of OPH[a]

[OPH] (μg/mL)	method[b]	$\Delta G1_W$ (kcal/mol)	$\Delta G2_W$ (kcal/mol)	m_1 (kcal mol^{-1} M^{-1})	m_2 (kcal mol^{-1} M^{-1})	$Y_{N°}$	$Y_{U°}$	Y_I	b_1	b_2
125	Fl	4.25 ± 0.08	34.0 ± 4.3	0.90 ± 0.18	4.07 ± 0.58	310 ± 5	170 ± 100	239 ± 5	5 ± 2	−8 ± 12
68	Fl	4.11 ± 0.14	35.9 ± 0.9	0.95 ± 0.02	3.95 ± 0.17	311 ± 7	140 ± 50	216 ± 7	12 ± 4	−4 ± 5
34	Fl	4.20 ± 0.25	34.6 ± 1.2	0.98 ± 0.05	4.80 ± 0.13	293 ± 4	110 ± 60	173 ± 12	18 ± 3	0 ± 1
13	Fl	4.11 ± 0.26	33.8 ± 1.7	1.13 ± 0.06	3.88 ± 0.19	280 ± 5	90 ± 70	132 ± 9	25 ± 3	3 ± 7
125	CD	4.40 ± 0.10	37.8 ± 1.3	0.91 ± 0.06	3.99 ± 0.06	7700 ± 200	1700 ± 200	2500 ± 300	80 ± 20	0
68	CD	4.55 ± 0.17	36.5 ± 0.8	0.94 ± 0.05	4.39 ± 0.02	7900 ± 300	1600 ± 200	2700 ± 200	70 ± 20	0
34	CD	4.83 ± 0.09	36.9 ± 0.8	1.09 ± 0.08	4.62 ± 0.09	7700 ± 300	1600 ± 400	2500 ± 300	−100 ± 80	0
13	CD	4.09 ± 0.10	39.0 ± 1.4	0.97 ± 0.08	4.69 ± 0.09	7300 ± 400	1900 ± 300	2500 ± 600	120 ± 200	0
average[c]	Fl + CD	4.32 ± 0.26	36.1 ± 1.9	0.98 ± 0.08	4.30 ± 0.37	–	–	–	–	–
global[d]	CD	4.33 + 0.03	37.8 ± 2.1	0.95 ± 0.02	4.55 ± 0.04	7600 ± 300	1800 ± 300	2600 ± 500	80 ± 100	0

[a] The data sets from each of the protein denaturation curves were analyzed individually as described in the text to afford measures of the cardinal thermodynamic parameters (ΔG_W and m) for each of the two transitions. In addition, the five parameters describing the spectroscopic signal (Y_x) and the denaturant dependence to that parameter (b_x) are given. Errors are determined from the nonlinear least-squares analysis (see text for details). For the fluorescence-monitored transitions, the last five parameters are relative fluorescence intensities whereas for the transitions monitored by circular dichroism, the spectroscopic values are absolute measures of the mean residue ellipticity at 230 nm, expressed in deg cm^2 dmol^{-1}. [b] Fl, fluorescence; CD, circular dichroism. [c] The average and standard deviation of the eight individual analyses of the urea denaturation curves listed above. [d] Results from the "global analysis" of the four CD-monitored denaturation curves. See the text for details and additional information.

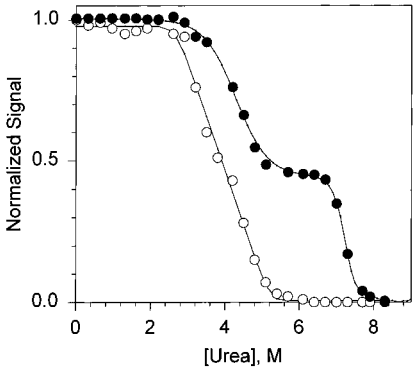

FIGURE 5: Relationship between equilibrium unfolding followed by fluorescence and enzymatic activity. Urea-induced unfolding of OPH (125 μg/mL) was measured by fluorescence emission (●) at 320 nm with excitation at 278 nm and by enzymatic activity (○). Theoretical curve for fluorescence emission was calculated as described in the legend for Figure 4. Theoretical curve for enzymatic activity was obtained from a least-squares fit of a two-state unfolding transition (Pace & Scholtz, 1996) to the data using an IBM version of Origin.

Table 2: Thermodynamic Parameters Obtained from Measurements of Loss of Enzymatic Activity[a]

[OPH] (μg/mL)	ΔG_W (kcal/mol)	m (kcal mol^{-1} M^{-1})	[urea$_{1/2}$] (M)
125	4.3	1.10	3.90
68	4.6	1.21	3.85
34	3.5	0.98	3.60
13	4.8	1.28	3.75
average	4.3 ± 0.5	1.14 ± 0.13	3.77 ± 0.13

[a] The analysis assumed a simple two-state denaturation process as described in the text. The errors on the individual values are m, ±0.10 kcal mol^{-1} M^{-1}; [urea$_{1/2}$]; ±0.05 M.

protein concentration-independent (Figure 4). The second unfolding transition (4.5 M−8 M urea) was strongly concentration-dependent, suggesting that subunit dissociation occurred in this transition. Clearly, this step was bimolecular and the intermediate formed prior to subunit dissociation; our model involving a dimeric intermediate is consistent with these data.

The results of our data analysis were consistent from both spectral methods, and at different protein concentrations (Table 1). The parameters that govern the thermodynamic

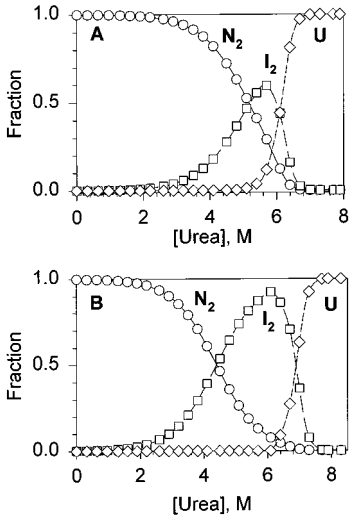

FIGURE 6: Fractions of N_2, I_2, and U as a function of urea concentration. The fractions of native (N_2), intermediate (I_2), and unfolded (U) protein were calculated as a function of urea concentration for protein concentrations of 12.5 μg/mL (A) and 125 μg/mL (B) using data in Table 1 and equations found under Experimental Procedures: (○) native OPH; (□) dimeric intermediate; (◇) unfolded OPH.

distribution of three species, native enzyme, intermediate, and denatured subunits, at each urea concentration are shown in Table 1, and the distributions are plotted in Figure 6, where, for clarity, only the lowest and the highest protein concentrations are shown. The fraction of protein in the intermediate form is largest for the highest protein concentration, about 93% at 6 M urea and 125 μg/mL. This shows that the intermediate is well-populated at equilibrium and is sufficiently stable to allow spectroscopic analysis.

The m values obtained in our study (Table 1) can be related to the global changes occurring during unfolding of OPH in urea. Denaturant m values, the dependence of the free energy of unfolding on denaturant concentration, were collected for a large set of proteins (*31*). In that study, the m value was found to correlate strongly with the amount of protein surface exposed to solvent upon unfolding. We used this relationship to estimate the change in accessible surface area, ΔASA, during the first and second unfolding transitions of OPH based on our observed m values, $m_1 = 0.95$ kcal mol^{-1} M^{-1} and $m_2 = 4.55$ kcal mol^{-1} M^{-1}. The ΔASA's were 5400

and 36 000 Å^2, respectively, for the two transitions. This is consistent with the observation that subunit dissociation and the conversion of the intermediate to denatured monomers occurred in the second transition, where the most exposure of surface area would be expected. Based on the *m* values and the relative Δ*ASA*, only 15−20% of the total change occurs in the $N_2 \leftrightarrow I_2$ transition. This is substantially smaller than the absolute changes in the fluorescence and CD signals. Therefore, the $N_2 \leftrightarrow I_2$ conformational change results in less than 20% change in the accessible surface area, but a significantly larger change in Trp exposure and α-helix content. We hope to characterize the structure of I_2 more completely in future studies.

The fluorescence emission spectrum of the intermediate form in 1.6 M GdmCl shifted slightly to a longer wavelength (Figure 3A) than native OPH. Both the fluorescence intensity and λ_{max} values differ for the three states. The λ_{max} values indicate that the Trp residues are, on average, in a more polar environment in the intermediate and that the Trps are completely exposed to solvent in the unfolded state (*37*). The circular dichroism of the intermediate in the far-UV (222 nm) is decreased by about 50%, suggesting partial unfolding, and disruption of considerable secondary structure (Figure 3B). This decrease may represent a local loss of secondary structure in an exposed part of the protein, perhaps in the α-helices (Figure 1). However, the change in CD from N_2 to I_2 may not reflect just secondary structure content, since aromatic residues also contribute to the CD in this region. Therefore, without further structural characterization, it is not possible to contribute the loss of CD signal to the disappearance of any secondary structure elements. It is quite amazing, however, that OPH remains a dimer with such a large change in the far-UV CD.

There is an entropic cost paid to form a dimer, but it is clear that this is more than offset by the gain in stability from forming the dimer interface. Using information from crystal structures, and experimentally determined Δ*G* values for subunit association, both Horton and Lewis (*38*) and Nussinov's group (*39*, *40*) have considered the energetics of subunit associations in detail. For most protein associations, the hydrophobic effect makes the dominant contribution to the stability, and this is also true with OPH. Using the crystal structure and Lee and Richard's algorithm (*41*), we estimate that 2200 Å^2 of nonpolar surface is buried on forming the dimer. [The corresponding burial of polar surface is ≈990 Å^2, so about 11% of the monomer surface is involved in the intersubunit interface (*19*).] Karplus (*42*) recently suggested that a value of 25 cal mol^{-1} Å^{-2} of nonpolar surface should be used to estimate the contribution of nonpolar group burial to stability, and this is the same value recommended by Horton and Lewis (*38*). This leads to an estimate of 55 kcal/mol for the contribution of the hydrophobic effect to OPH dimer stability. Based on the estimates of Horton and Lewis (*38*) and more recent estimates (*43*), the eight hydrogen bonds and the single salt bridge at the interface probably contribute about 15 kcal/mol to the stability, considerably less than the hydrophobic effect. In contrast, Horton and Lewis estimate that the entropic cost of the loss of translational and rotational degrees of freedom is only 6.2 ± 2.2 kcal/mol. Thus, these rough estimates suggest that intersubunit interactions probably make a net contribution of more than 60 kcal/mol to the stability of OPH. This is greater than the overall conformational stability that we observe, ≈40 kcal/mol. Taking this into account, it is less surprising that the dimer can remain intact when a sizable portion of the OPH molecule is unfolding.

Our data show that OPH is a very stable protein with a total standard state free energy change for dissociation and subunit unfolding of ≈40 kcal/mol, and a apparent T_m of ≈75 °C. This is the greatest conformational stability reported for any dimeric protein. Several of the dimeric proteins reported by Neet and Timm (*36*) have standard state stabilities in the range of 20−30 kcal/mol, and Trp repressor, a homodimer, and bacterial luciferase, a heterodimer, have stabilities of ≈24 kcal/mol (*10*, *11*). As discussed above, OPH probably gains more than 60 kcal/mol in stability by forming a dimer. Thus, it is now clear that oligomeric proteins (*36*, *38*, *39*) are generally more stable than monomeric proteins, and that the stability that they gain from intersubunit interactions is more than enough to offset the entropic cost of forming the oligomeric state. In addition, OPH probably gains considerable stability from the metals that are bound by the folded protein. This is currently being investigated in our laboratory.

We have established conditions that allow a more extensive investigation of the conformational stability of OPH. The existence of a stable, dimeric intermediate will allow direct investigations into the structural aspects of OPH dimer formation and denaturation. Detailed information about the structure of the interface and the stability of the OPH dimer can be useful in engineering novel proteins with desirable characteristics for bioremediation and for enhancing their stability under a variety of environmental conditions important in remediation technology.

ACKNOWLEDGMENT

We thank Kevin Shaw for generating Figure 1, Steve Raso for help with data analysis, and Eric J. Hebert for analyzing the solvent accessibility and the hydrogen bonding of OPH.

REFERENCES

1. Zetina, C. R., and Goldberg, M. E. (1980) *J. Mol. Biol. 137*, 401−414.
2. Pabo, C. O., Sauer, R. T., Sturtevant, J. M., and Ptashne, M. (1979) *Proc. Natl. Acad. Sci. U.S.A. 76*, 1608−1612.
3. Banik, U., Saha, R., Mandal, N. C., Bhattacharyya, B., and Roy, S. (1992) *Eur. J. Biochem. 206*, 15−21.
4. Herold, M., and Kirschner, K. (1990) *Biochemistry 29*, 1907−1913.
5. Leistler, B., Herold, M., and Kirschner, K. (1992) *Eur. J. Biochem. 205*, 603−611.
6. Mei, G., Rosato, N., Silva, N., Jr., Rusch, R., Gratton, E., Savini, I., and Finazzi-Agro, A. (1992) *Biochemistry 31*, 7224−7230.
7. Aceto, A., Caccuri, A. M., Sacchetta, P., Bucciarelli, T., Dragani, B., Rosato, N., Federici, G., and Di Ilio, C. (1992) *Biochem. J. 285*, 241−245.
8. Sacchetta, P., Aceto, A., Bucciarelli, T., Dragani, B., Santarone, S., Allocati, N., and DiIlio, C. (1993) *Eur. J. Biochem. 215*, 741−745.
9. Blackburn, M. N., and Noltmann, E. N. (1981) *Arch. Biochem. Biophys. 212*, 162−169.
10. Clark, A. C., Sinclair, J. F., and Baldwin, T. O. (1993) *J. Biol. Chem. 268*, 10773−10779.
11. Gloss, L. M., and Matthews, C. R. (1997) *Biochemistry 36*, 5612−5623.
12. Donarski, W. J., Dumas, D. P., Heitmeyer, D. P., Lewis, V. E., and Raushel, F. M. (1989) *Biochemistry 28*, 4650−4655.
13. Lewis, V. E., Donarski, W. J., Wild, J. R., and Raushel, F. M. (1988) *Biochemistry 27*, 1591−1597.

14. Dumas, D. P., Wild, J. R., and Raushel, F. M. (1989) *Biotech. Appl. Biochem. 11*, 235−243.
15. Dumas, D. P., Durst, H. D., Landis, W. G., Raushel, F. M., and Wild, J. R. (1990) *Arch. Biochem. Biophys. 277*, 155−159.
16. Hoskin, F. C. G., Walker, J. E., Dettbarn, W., and Wild, J. R. (1995) *Biochem. Pharmacol. 49*, 711−715.
17. Omburo, G. A., Kuo, J. M., Mullins, L. S., and Raushel, F. M. (1992) *J. Biol. Chem. 267*, 13278−13283.
18. McDaniel, C. L., Harper, L. L., and Wild, J. R. (1988) *J. Bacteriol. 1705*, 2306.
19. Benning, M. M., Kuo, J. M., Raushel, F. M., and Holden, H. M. (1994) *Biochemistry 33*, 15001−15007.
20. Benning, M. M., Kuo, J. M., Raushel, F. M., and Holden, H. M. (1995) *Biochemistry 34*, 7973−7978.
21. Vanhooke, J. L., Benning, M. M., Raushel, F. M., and Holden, H. M. (1996) *Biochemistry 35*, 6020−6025.
22. Lai, K., Dave, K. I., and Wild, J. R. (1994) *J. Biol. Chem. 269*, 16579−16584.
23. Lai, K., Stolowich, N. J., and Wild, J. R. (1995) *Arch. Biochem. Biophys. 318*, 59−64.
24. Lai, K., Grimsley, J. K., Kuhlmann, B. D., Scapozza, L., Harvey, S. P., DeFrank, J. J., Kolakowski, J. E., and Wild, J. R. (1996) *Chimia 50*, 49−51.
25. Kraulis, P. J. (1991) *J. Appl. Crystallogr. 24*, 946−950.
26. Lai, K. (1994) *Modification and Characterization of the Neurotoxic Substrate Specificity of Organophosphorus Hydrolase*, Ph.D. dissertation, Texas A&M University.
27. Pace, C. N., Shirley, B. A., and Thomson, J. A. (1989) in *Protein Structure, A Practical Approach* (Creighton, T. E., Ed.) pp 311−330, IRL Press, New York.
28. Pace, C. N., and Scholtz, J. M. (1996) in *Protein Structure: A Practical Approach* (Creighton, T. E., Ed.) pp 297−319, Oxford University Press, New York.
29. Greene, R. F., and Pace, C. N. (1974) *J. Biol. Chem. 249*, 5388−5393.
30. Ahmad, F., and Bigelow, C. C. (1982) *J. Biol. Chem. 257*, 12935−12938.
31. Myers, J. K., Pace, C. N., and Scholtz, J. M. (1995) *Protein Sci. 4*, 2138−2148.
32. Santoro, M. M., and Bolen, D. W. (1988) *Biochemistry 27*, 8063−8068.
33. Johnson, M. L., and Frasier, S. G. (1985) *Methods Enzymol. 117*, 301−342.
34. Bowie, J. U., and Sauer, R. T. (1989) *Biochemistry 28*, 7139−7143.
35. Liang, H., and Terwilliger, T. C. (1991) *Biochemistry 30*, 2772−2782.
36. Neet, K. E., and Timm, D. E., (1994) *Protein Sci. 3*, 2167−2174.
37. Schmid, F. X. (1996) in *Protein Structure: A Practical Approach* (Creighton, T., Ed.) 2nd ed., pp 261−298, Oxford University Press, New York.
38. Horton, N., and Lewis, M. (1992) *Protein Sci. 1*, 169−181.
39. Tsai, C.-J., and Nussinov, R. (1997) *Protein Sci. 6*, 24−42.
40. Tsai, C.-J., Lin, S. L., Wolfson, H. J., and Nussinov, R. (1997) *Protein Sci. 6*, 53−64.
41. Lee, W. K., and Richards, F. M. (1971) *J. Mol. Biol. 55*, 379−400.
42. Karplus, P. A. (1997) *Protein Sci. 6*, 1302−1307.
43. Myers, J. K., and Pace, C. N. (1996) *Biophys. J. 71*, 2033−2039.

BI971596E